



# The New Composite Solar Flare Index from Solar Cycle 17 to Cycle 24 (1937 – 2020)

Victor Manuel Velasco Herrera<sup>1</sup> · Willie Soon<sup>2,3</sup> · Štefan Knoška<sup>4</sup> · Jorge Alberto Perez-Peraza<sup>1</sup> · Rodolfo G. Cionco<sup>5</sup> · Sergey M. Kudryavtsev<sup>6</sup> · Shican Qiu<sup>7</sup> · Ronan Connolly<sup>8</sup> · Michael Connolly<sup>9</sup> · Michal Švanda<sup>10</sup> · José Acosta Jara<sup>11</sup> · Giovanni Pietro Gregori<sup>12</sup>

Received: 24 January 2022 / Accepted: 1 July 2022  
© The Author(s), under exclusive licence to Springer Nature B.V. 2022

## Abstract

The chromosphere is a highly dynamic outer plasma layer of the Sun. Its physical processes accounting for the variability are poorly understood. We reconstructed the solar chromospheric flare index (SFI) to study the solar chromospheric variability from 1937 to 2020. The new SFI database is a composite record of the Astronomical Institute Ondřejov Observatory of the Czech Academy of Sciences from 1937–1976 and the records of the Kandilli Observatory of Istanbul, Turkey from 1977–2020. The SFI records are available in daily, monthly, and yearly resolutions. We carried out the time-frequency analyses of the new 84-year long SFI records using the wavelet transform. We report the periodicities of 21.88 (Hale cycle), 10.94 (Schwabe cycle), 5.2 (quasi-quinquennial cycle), 3.5, 1.7, 1, 0.41 (or 149.7 days, Rieger cycle), 0.17 (62.1 days), 0.07 (25.9 days, solar rotational modulation) years. All these periodicities seem always present and persistent throughout the observational interval. Thus, we suggest that there is no reason to assume these solar periodicities are absent from other solar cycles. Time variations of the amplitude of each oscillation or periodicity were also studied using the inverse wavelet transform. We found that for the SFI the most active flare cycles over the record were Cycles 17, 19, and 21, while Cycles 20, 22, 23, and 24 were the weakest ones with Cycle 18 was intermediate in flare activity. This shows several differences to the equivalent relationships for solar activity implied by sunspot number records. Furthermore, this confirms that solar activity trends and variability in the chromosphere as captured by SFI are not necessarily the same as those of the Sun's photosphere, as implied by the sunspot number activity records, for instance. We have also introduced a new signal/noise wavelet coherence metric to analyze two different chromospheric indices available (i.e. the SFI and the disk-integrated chromospheric Ca II K activity

---

Š. Knoška formerly of the Astronomical Institute of the Slovak Academy of Sciences, Tatranská Lomnica, 059 60, Slovak Republic.

---

R. Connolly is an independent scientist, Dublin, Ireland.

---

M. Connolly is an independent scientist, Dublin, Ireland.

---

IDASC (CNR), now merged into IMM (CNR).

---

Giovanni Pietro Gregori is retired.

---

Extended author information available on the last page of the article

indices) and to quantify the differences and similarities of the oscillations within the solar chromosphere. Our findings suggest the importance of carrying out additional co-analyses with other solar activity records to find physical inter-relations and connections between the different solar layers from the photosphere, the chromosphere to the corona.

**Keywords** Solar flare · Bright chromospheric eruptions · Solar magnetic and chromospheric activity · Wavelet analysis · Bayesian probabilistic quantification of solar activity

## 1. Introduction

Richard Christopher Carrington (1859) reported that on the morning of Thursday, September 1, 1859 when he was making his routine observations of the shapes and positions of sunspots from the Redhill Observatory, England (Carrington, 1863), he witnessed an exceedingly rare appearance of a transient phenomenon on the surface of the Sun. Two patches of intensely bright white light broke out. Luckily, Carrington's observation was also independently noted as "a very brilliant star of light" on the Sun's surface, described in Hodgson (1859). In addition, there were no major changes in the sunspot group that Carrington had drawn before this explosive emission occurred. Therefore, this emission could not have originated from the underlying sunspot activity, and the detailed mechanisms are still a major research topic (see, e.g., Lin, Soon, and Baliunas, 2003; Hao et al., 2017; Song et al., 2020).

The development of the physics of solar flares and/or coronal mass ejections did not progress quickly nor systematically after Carrington and Hodgson's pioneering observations in part due to the rarity of white-light flares and the lack of instruments to generate images or to capture the dynamical developments of the rapid manifestation of a solar flare transient (see, e.g., Lin, Soon, and Baliunas, 2003). It is also obvious that not all solar flares are highly energetic white-light flares. Another highly probable white-light flare in historical times was the one described as a "flash of lightning" near a sunspot by Stephen Gray (1666–1736) on December 27, 1705, coincidentally timed nearing the end of the infamous Maunder Minimum, an interval of anomalously weak sunspot activity (Clark and Murdin, 1979; Soon and Yaskell, 2003; Velasco Herrera et al., 2022a). Neidig and Cliver (1983) reported a total of 57 solar white-light flares between 1859 and 1982, but only four occurred in the 19th century: September 1, 1859; November 13, 1872; June 17, 1891; July 15, 1892. Recently, Vaquero, Vazquez, and Sanchez Almeida (2017) uncovered another new evidence for a white-light flare on September 10, 1886 observed by the amateur astronomer Juan Valderrama y Aguilar (1869–1912). Eddy (1974) demonstrated a most convincing early candidate for a coronal mass ejection during the total solar eclipse event of July 18, 1860.

Solar flares are abrupt processes that release large amounts of radiant and charged-particle energy (see, e.g., Fletcher et al., 2011; Shibata and Magara, 2011; Kusano et al., 2020; Li et al., 2022) that affect the state and condition of the Earth's magnetosphere and upper atmosphere (see, e.g., Krauss et al., 2012; Velasco Herrera et al., 2018; Zhang et al., 2021; Miteva and Samwel, 2022). The observations of solar flares are therefore important for the scientific understanding of solar activity, space weather, and Sun-Earth physical relations. Unfortunately, the "exact" quantitative value of the total energy produced by flares cannot be determined. So, Link and Kleczek (1949) and Kleczek (1952) have introduced, using observations with an  $H\alpha$  (6563 Å) filter, the solar flare index (SFI) as:

$$SFI = i \cdot t. \quad (1)$$

The SFI parameter gives an approximation of the total amount of energy emitted by each eruption, where  $t$  is the minimum duration of the eruption and  $i$  first introduced by Link and Kleczek (1949) as “importance” (in French; for the optical ranking of the solar eruption), was later called “power” in Czech and Russian by Kleczek (1952) (*mohutnost* and *мощность*, respectively).

We want to highlight that since the variable SFI expresses the value of the radiated energy of each eruption, then according to Eq. 1, SFI is the product of the power ( $i$ ) and the eruption interval ( $t$ ). So the physical sense of  $i$  constitutes the eruptive power, while the term “importance” does not really even adequately express the physical sense of a solar flare. So in this work, we will adopt the term “power” to represent the variable  $i$ .

Richardson (1944) questioned the change in terminology from bright chromospheric eruptions to solar flares and mentioned that the strongest reason for that switch could be that with the word flare one can concisely capture “the three most outstanding features of the phenomenon: its sudden appearance, great brilliancy, and rapid variations in intensity.” Richardson also pointed out that the word flare was first used by McNish (1937a) in the article “The Atmosphere’s Electrical Fringe” when McNish wrote that “Solar eruptions cause the fade-out of high-frequency radio signals on the daylight side of the Earth, lasting at times from a few minutes to over an hour... [A]bout 100 such cases have been reported. About half of these cases occurred at times when bright flares of hydrogen light were visible on the Sun, revealed by a special instrument called a spectrohelioscope. It is believed that all of these fade-outs occur simultaneously with solar eruptions – absence of solar observations some times accounting for the failure of any astronomer to report observation of a flare.” Here, we wish to correct this mis-statement by Richardson (1944) because one can find an earlier mention of a “solar flare” in McNish’s publication in *Physical Review*, which was submitted on March 25, 1936 as McNish (1937b) while the popular magazine article by McNish was dated October 24, 1937.

Different studies have partially analyzed the SFI variations with different temporal resolutions for the entire solar disk and each of the solar hemispheres. For example, Švestka (1956) performed a monthly statistical analysis of chromospheric flares from 1937 to 1952. Later, Knoška (1985) analyzed the SFI annually from 1937 to 1976, covering four solar cycles (i.e. from Cycle 17 to 20). For Solar Cycles 20 to 24, different spectral studies of the SFI have been systematically carried out (Özgüç and Ataç, 1989; Özgüç, Ataç, and Rybák, 2002; Ataç and Özgüç, 2006; Mendoza and Velasco Herrera, 2011; Velasco Herrera et al., 2018; Özgüç et al., 2021). In this work, we have reconstructed the SFI with a daily, monthly, and annual temporal resolution from 1937 to 1976 based on the pioneering observations at the Ondřejov Observatory. In addition, we have used the catalogue of SFI activity from the Kandilli Observatory between 1977 to 2020 to provide the complete composite of the SFI time series from Solar Cycle 17 to Solar Cycle 24, roughly covering the interval from 1937 – 2020.

## 2. Data and Methodology

### 2.1. Solar Flare Records

The solar flare index is related to explosive solar activity and indeed has been relatively well studied (e.g. Švestka, 1956; Knoška, 1985; Ataç, 1987; Özgüç and Ataç, 1989, 1994, 1996; Özgüç, Ataç, and Rybák, 2002; Ataç and Özgüç, 2006; Mendoza and Velasco Herrera, 2011; Velasco Herrera et al., 2018; Özgüç et al., 2021). The SFI has been analyzed in a

piecewise manner and somewhat discontinuously for different solar cycles. These analyses have been conducted for the entire solar disk as well as for individual hemispheres. This article studies the SFI for the entire solar disk from Solar Cycle 17 to Solar Cycle 24 or roughly the 1937–2020 interval.

In order to achieve this goal, the following catalogues of chromospheric flares are assembled to reconstruct the daily, monthly, and annual variations of the solar flare index for the entire solar disk between 1937 and 1976.

- i) Kleczek (1952), catalogue of chromospheric flares from 1937 to 1949.
- ii) Knoška and Letfus (1966), catalogue of chromospheric flares from 1950 to 1965.
- iii) Knoška and Petrášek (1984), catalogue of chromospheric flares from 1966 to 1976.

We also use the catalogue of chromospheric flares from 1977 to 2020 by Boğaziçi Üniversitesi, Kandilli Rasathanesi ve Deprem Araştırma Enstitüsü Astronomi Laboratuvarı.<sup>1</sup>

The spatial-temporal nature and the hemispheric asymmetry of the SFI with respect to and in relation to other solar activity metrics will be postponed for a future work.

## 2.2. Wavelet Time-Frequency Spectral Analysis

There are at least two types of analysis that allow to deduce information on solar activity and its spatial-temporal variations. One is the direct processing of the Sun's images in various wavelengths (digital, analogic, from the ground, and from space, among others), and the second is the processing of solar activity signals. Signal processing can be performed temporally and spectrally to find patterns and to deduce or infer the energy and power of solar phenomena. The detected signals allow the study and quantification of intrinsic properties such as their amplitude, wavelength, frequency, energy, and power, among others.

Solar information deduced from both the temporal and frequency spaces is equivalent, and is found in very different algebraic spaces with properties and operations often very well defined. There is no single methodology that can allow us to deduce and access all the necessary solar information. On some occasions, temporal spaces provide the necessary information to understand solar activity straightforwardly. On other occasions, this information is neither obvious nor well defined. Hence, it is necessary to look for clearer information in other spaces such as in the frequency space. In this work, we analyze the SFI time series using the wavelet transform, because we are interested in understanding the evolution of the periodicities over time. A general description is presented below.

There are different spectral methods to analyze the frequencies of a function (time series). For example, the Fourier transform should be used only when the frequencies contained in a function are present at any point in time (Fourier, 1822). Therefore, the amplitudes of the oscillations with these frequencies do not change in time (Fourier, 1822). In the case of the SFI, this requirement is clearly not fulfilled. A noisy spectral function can be obtained using the Fourier transform for data whose frequency changes with time. However, the noisy spectra are produced because a spectral analysis is applied to data that do not belong to the linear Hilbert space in  $L_2$  norm (LHS- $L_2$ , e.g., see Chapters 2 and 5 of Alabiso, 2015).

We apply the standard wavelet technique (Grossmann and Morlet, 1984) that is appropriate for studying non-stationary times series (Cappellotto et al., 2022; Orgeira et al., 2022; Velasco Herrera et al., 2022b), i.e. data that do not belong to LHS- $L_2$  norm, for example the SFI record. When there is a noisy spectrum, white noise is classically used to try to separate and distill the true frequencies from the random spurious ones. In our case, we will use

---

<sup>1</sup><https://astronomi.boun.edu.tr/>.

red noise (Gilman, Fuglister, and Mitchell, 1963). Torrence and Compo (1998) defined the wavelet transform as:

$$W_n(s) = \sum_{n'=0}^{N-1} x_{n'} \Phi^* \left( \frac{n' - n}{s} \right) \delta t, \tag{2}$$

where  $s$  is the dilation parameter (scale),  $n$  is the translation in time parameter, the  $*$  denotes complex conjugate,  $\Phi$  is the mother wavelet function, and  $\delta t$  is the resolution of the time series. Here we use the Morlet wavelet and the wavelet software provided by Torrence and Compo (1998),<sup>2</sup> Aguiar-Conraria, Azevedo, and Soares (2008),<sup>3</sup> Grinsted, Moore, and Jevrejeva (2004),<sup>4</sup> and Velasco Herrera et al. (2017).<sup>5</sup>

We acknowledge that the generalization of the standard Fourier transform for non-stationary signals in terms of the so-called short-time (or windowed) Fourier transform is also another suitable method (e.g. Kollath and Olah, 2009; Olah et al., 2016; Cappellotto et al., 2022; Orgeira et al., 2022).

### 2.2.1. Inverse Wavelet Spectral Analysis

We use the inverse wavelet (Torrence and Compo, 1998) equation to obtain the oscillations of SFI ( $y_n$ ) in the temporal coordinate:

$$y_n = \frac{\delta_j \delta t^{1/2}}{C_\delta \psi_o(0)} \sum_{j=j_1}^{j_2} \frac{\text{Re}(W_n(s_j))}{s_j^{1/2}}, \tag{3}$$

where  $j_1$  and  $j_2$  define the scale range of the specified spectral bands. For a Morlet wavelet,  $\delta_j = 0.6$ ,  $C_\delta = 0.776$ , and  $\psi_o(0) = \pi^{-1/4}$ .

### 2.2.2. Signal-to-Noise Wavelet Coherence

Coherence is an intrinsically frequency dependent function that was first introduced in signal analysis by Wiener (1930). The concept of coherence was introduced in wavelet spectral analysis (see, e.g., Torrence and Compo, 1998; Torrence and Webster, 1999). The classical wavelet squared coherency ( $\gamma^2$ ) is defined by Soon et al. (2019) in order to identify frequency bands within which two time series  $X$  and  $Y$  (i.e. the composite SFI and the composite chromospheric Ca II K time series for example) covary as:

$$\gamma^2(s, \tau) = \langle |W^{XY}(s, \tau)|^2 \rangle \ominus \langle |\Omega(s, \tau)|^2 \rangle, \tag{4}$$

with

$$W^{XY}(s, \tau) = W^X(s, \tau) \otimes W^{*Y}(s, \tau),$$

$$\langle |\Omega_g(s, \tau)|^2 \rangle = \langle s^{-1} |W^X(s, \tau)|^2 \rangle \otimes \langle s^{-1} |W^Y(s, \tau)|^2 \rangle,$$

<sup>2</sup><https://paos.colorado.edu/research/wavelets/software.html>.

<sup>3</sup><https://sites.google.com/site/aguiarconraria/joanasoares-wavelets/the-astoolbox>.

<sup>4</sup><https://noc.ac.uk/business/marine-data-products/cross-wavelet-wavelet-coherence-toolbox-matlab>.

<sup>5</sup><https://www.geofisica.unam.mx/radiacion-solar/estructura.html>.

where  $\otimes$  and  $\ominus$  are the Hadamard multiplication of matrices and the Hadamard division of matrices, respectively (see Soon et al., 2019, for more details on the method),  $\langle \cdot \rangle$  represents the temporal and frequency average (e.g. Torrence and Compo, 1998; Torrence and Webster, 1999; Grinsted, Moore, and Jevrejeva, 2004; Velasco Herrera et al., 2017; Soon et al., 2019), and  $*$  denotes the complex conjugation.  $W^{XY}(s, \tau)$  is the cross wavelet (Hudgins, Friehe, and Mayer, 1993) that is computed to study the co-varying nature of the time series; it measures the synchronization in phase and/or frequency of two phenomena ( $X$  and  $Y$ ).  $W^X$  and  $W^Y$  are the wavelet transforms of the two time series  $X$  and  $Y$ .

The instantaneous relative phase difference in the classical wavelet squared coherence ( $\phi$ ), the global time-averaged wavelet coherence spectrum ( $G_{\gamma^2}$ ), and the global frequency-averaged wavelet coherence spectrum ( $G_\phi$ ) are defined by Soon et al. (2019) respectively as follows:

$$\phi(s, \tau) = \tan^{-1} (\mathbf{Im}[W^{XY}(s, \tau)] \ominus \mathbf{Re}[W_g^{XY}(s, \tau)]), \quad (5)$$

$$G_{\gamma^2} = \sum_t \gamma^2(s, \tau),$$

$$G_\phi = \sum_\phi \phi(s, \tau).$$

The coherence between two time series (i.e. the composite SFI and the composite chromospheric Ca II K) in a physical system (i.e. the solar chromosphere) can be calculated through the relation signal/noise, i.e. the signal-to-noise ratio is the ratio between the spectral power of a signal and the spectral power of the background noise. In our case, the noise is any unwanted disturbance that degrades the quality of the chromospheric activity variation signal. We define the signal/noise wavelet coherence ( $\hat{\Phi}_{s/n}$ ) as:

$$\hat{\Phi}_{s/n} = \frac{\gamma^2}{1 - \gamma^2}, \quad (6)$$

where  $\gamma^2$  is the classical wavelet squared coherence.

### 2.3. SFI Power Anomalies

The power ( $P$ ) is defined as the ratio of energy transfer per unit time (Feynman, Leighton, and Sands, 1963; Landau and Lifshitz, 1988). We use the standardized power anomaly ( $\hat{P}$ ) to quantify whether an SFI cycle is strong or weak; it is defined (Velasco Herrera, Mendoza, and Velasco Herrera, 2015; Soon et al., 2019; Velasco Herrera, Soon, and Legates, 2021; Orgeira et al., 2022) as:

$$\hat{P}_i = \frac{P_i - \langle P_i \rangle}{\sigma_i}, \quad (7)$$

where  $\langle P_i \rangle$  is the mean value and  $\sigma_i$  is the standard deviation of the SFI power in the solar cycle  $i$  ( $i = 17, 18, \dots, 24$ ).

## 2.4. Bayesian Inference

We apply the Bayesian inference machine learning model (see Suykens et al., 2005; Soon et al., 2019; Velasco Herrera, Soon, and Legates, 2021; Velasco Herrera et al., 2022a,b, for technical descriptions about the method) obtained from the original composite SFI record between 1937 and 2020 in order to provide a probabilistic estimate of the SFI uncertainties. We apply Bayes theorem (Bayes, 1763) to calculate this uncertainty; the Bayesian probability can be expressed as follows:

$$p(f|D) = \frac{p(D|f)}{p(D)} p(f), \quad (8)$$

with

$$f = \sum_{k=1}^n W_k D^k + B, \quad (9)$$

where  $f$  is the least-squares support-vector machine (LS-SVM) model.  $D^k$  in our case is the SFI at time  $k$  ( $k = 1, \dots, n$ ),  $W$  is the weighting factor, which in turn has a functional dependence on  $D^k$  and  $B$  is the bias term.

## 3. Results and Discussion

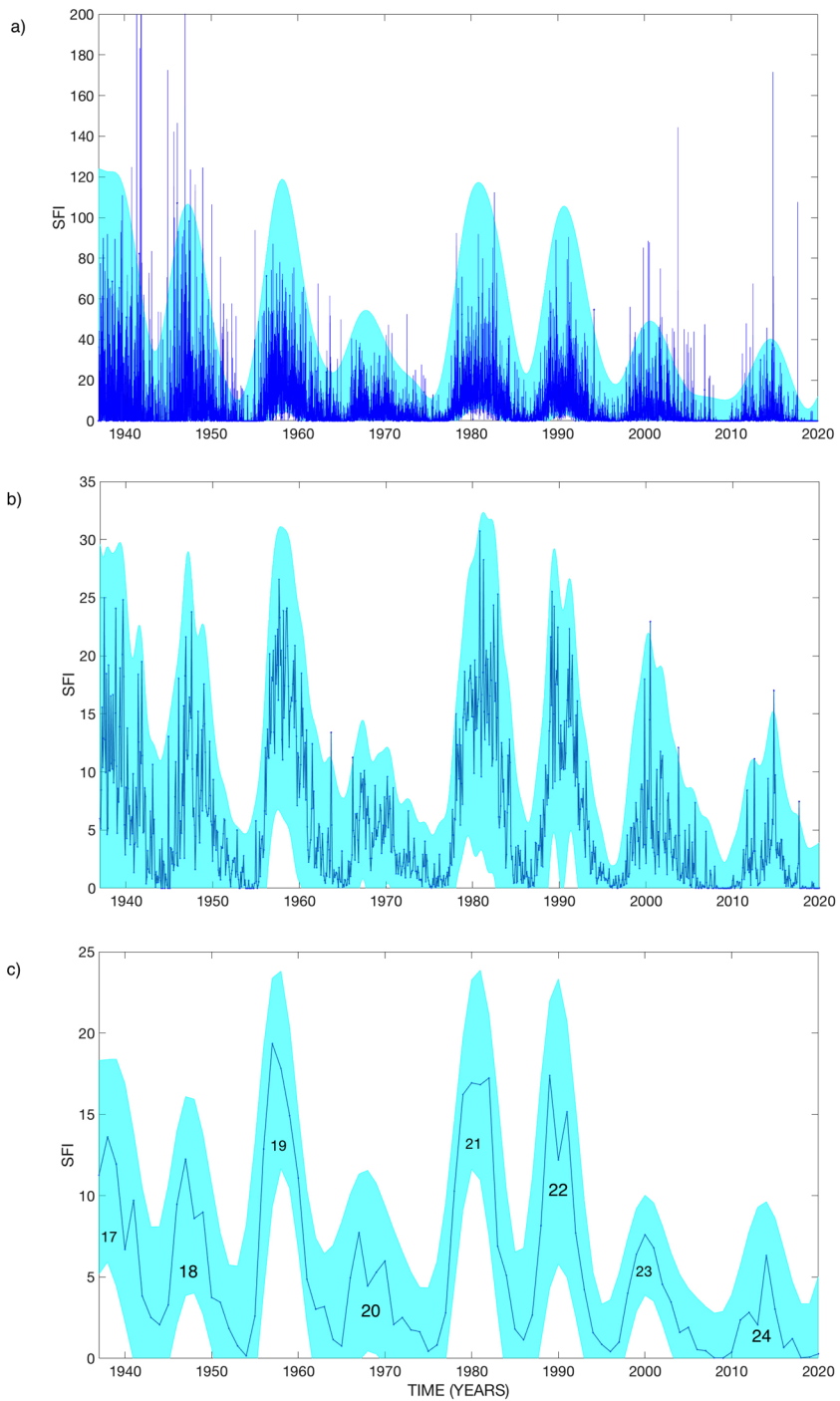
### 3.1. SFI Composite Record

Figure 1 shows the daily, monthly, and annual variations of the SFI from 1937 to 2020. All three time series display unique time variations and have SFI chromospheric activity cycle shapes and morphologies that are not trivial and not directly reflecting any one-to-one correspondence to the photospheric records like the sunspot activity datasets. In addition, from both Figures 1 and 2, we note that the relative amplitude of the SFI peaks during the maxima of the 11-year solar activity cycles are often different from other solar activity metrics, especially sunspot records.

Since it is impossible to calculate the exact value of the total integrated energy produced by solar flare eruptions (Link and Kleczek, 1949; Kleczek, 1952), we propose that the solar flare uncertainty should be considered and treated as a probabilistic estimation problem (Velasco Herrera, Soon, and Legates, 2021; Velasco Herrera et al., 2022a). Similarly, Camporeale (2019) has suggested that it is necessary to change the paradigms in solar activity research from an exact approach to a probabilistic one with reliable uncertainties. In Figure 1, the blue shaded area represents the 95% confidence intervals of the Bayesian SFI model.

#### 3.1.1. Comparison Between Composite SFI and Other Activity Indices from the Sun's Photosphere and Chromosphere

Several studies have emphasized that the term solar activity, actually comprises a multitude of different aspects of solar activity, and that often there can be subtle differences in the trends and variability of each aspect within and between consecutive solar cycles (Hoyt and Schatten, 1993; Livingston, 1994; Soon, Connolly, and Connolly, 2015; Connolly et al.,



**Figure 1** Time variations of the SFI (blue line) on (a) daily, (b) monthly, and (c) annual basis for Cycles 17–24 (1937–2020). The blue shaded area represents the 95% confidence interval of Bayesian model estimates of SFI values.



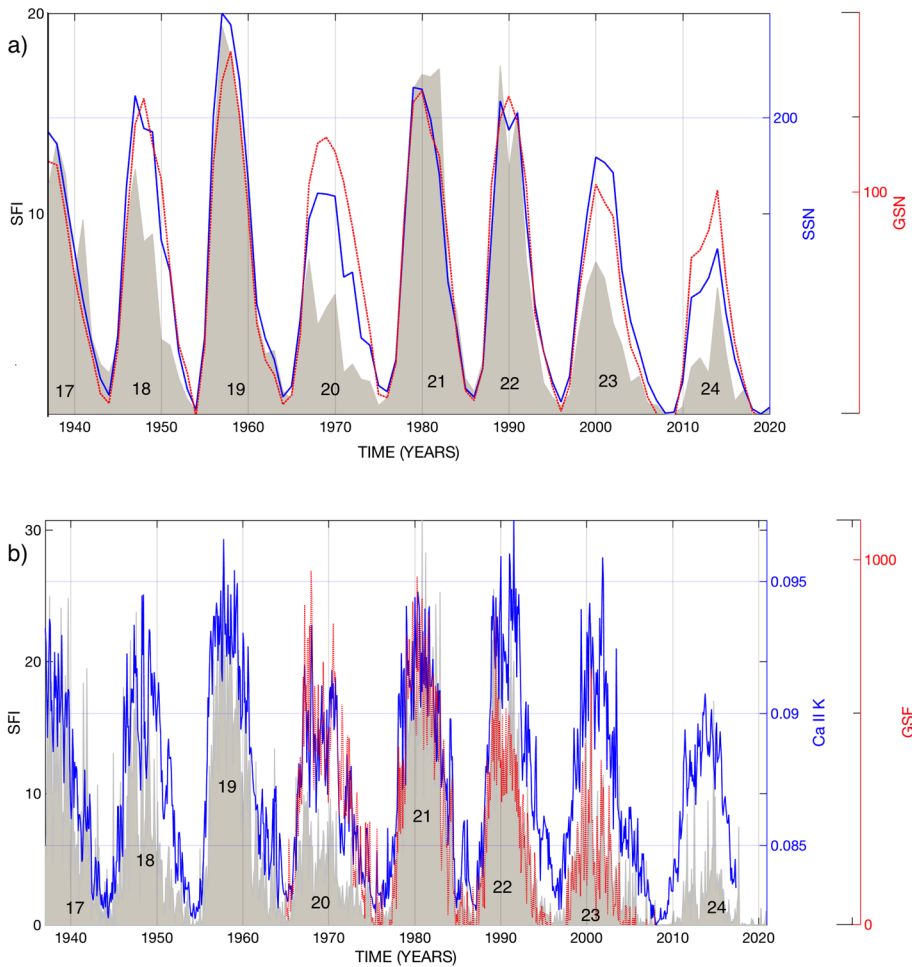


**Figure 2** Comparison between chromospheric SFI records and other activity indices from the Sun's photosphere and chromosphere from 1937 to 2020. **a)** Annual records of the composite SFI shown by the grey area, group sunspot numbers (GSN, Velasco Herrera et al., 2022a) indicated by the red line, and sunspot numbers (SSN V2, Clette et al., 2014) by the blue solid line. **b)** Monthly records of composite SFI (shown as a grey area), the disk-integrated composite chromospheric Ca II K time series (e.g. Bertello et al., 2016) shown by the blue solid line and grouped solar flare (GSF, from Deng, Mei, and Wang, 2020) by the red dotted line.

2021). Therefore, after obtaining the new composite SFI record, it can be useful to compare it to other solar photospheric and chromospheric activity indices.

Figure 2a shows the yearly comparison between the solar chromospheric ( $H\alpha$ , 6563 Å) flare index and two indicators of sunspot activity cycles. The comparison shows that the annual variation of the chromospheric SFI is roughly in phase with the solar cycle of the photosphere, represented by the sunspot number (SSN) and group sunspot number (GSN, recently reconstructed by Velasco Herrera et al., 2022a). However, while the relative amplitudes of each of the peaks are broadly similar for Cycles 17, 19, 21, and 22, there are notable differences for Cycles 18, 20, 23, and 24.

Figure 2b compares the monthly chromospheric SFI composite (shown as a grey area) to: (i) the monthly disk-integrated chromospheric Ca II K time series (e.g. Bertello et al., 2016; Egeland et al., 2017)<sup>6</sup> indicated by a blue line and (ii) the monthly grouped solar flares (GSF, e.g. Deng, Mei, and Wang, 2020)<sup>7</sup> shown by the red line. As the above analysis shows, there is a great similarity in the amplitude for Solar Cycles 21 and 22 between the three solar indices (SFI, Ca II K, and GSF). Furthermore, the activity morphology between SFI and Ca II K is very similar for Solar Cycles 17, 18, 19, 21, and 22. However, there are clear differences between these indices for Solar Cycles 20, 23, and 24 – although, the activity shape of Solar Cycle 20 is similar between GSF and Ca II K. This comparison between the three solar indices shows that the Sun’s chromosphere is a highly dynamic plasma layer, and the physical processes that explain the variability are little known and poorly understood, so it is necessary to perform a more in-depth analysis.

We want to highlight that the comparison between the various solar photospheric and chromospheric indices reveals both differences and similarities that exist between these two solar layers when using different resolutions (annual and monthly). This emphasizes the importance of considering multiple aspects of solar activity when studying solar variability (Hoyt and Schatten, 1993; Livingston, 1994; Soon, Connolly, and Connolly, 2015; Connolly et al., 2021).

The previous analysis considers solar variability on annual (Figure 2a) and monthly (Figure 2b) timescales. However, the solar flare index (SFI) is related to the explosive solar activity, which comprises abrupt processes that release large amounts of radiative and particle energy. Therefore, for this index, it is probably more insightful to consider the variation on a daily timescale. Therefore, we analyze the power of the SFI variation in each individual solar cycle and compare it with the activity power of the solar photosphere adopting the recent SSN V2 record of Clette et al. (2014).

### 3.1.2. Power Anomalies of the SFI Composite

To support and quantify our qualitative claim, we calculate the standardized power anomaly from the daily SFI composite and the SSN records for each solar cycle. Figure 3 shows the SFI and SSN power anomalies for Solar Cycles 17–24. The SFI power anomaly shown in Figure 3b features Cycles 17, 19, and 21 as the active flare cycles, while Cycles 20, 22, 23, and 24 are the weakest flare cycles and Cycle 18 is the intermediate flare cycle.

Although there are similarities between the two aspects of solar activity, there are also several marked differences. While the power anomalies show that Solar Cycle 19 is the most active in the solar photosphere, the most active SFI in the solar chromosphere is Solar Cycle 17. Also, while in the solar photosphere, the power anomalies are positive for Solar Cycle 17, they are negative in the photosphere. The situation is reversed for Solar Cycle 22. In the solar photosphere it is positive, but it is negative in the solar chromosphere.

These results help to illustrate the difference between photospheric and chromospheric solar activity and perhaps add insights to the nature of the magnetic heating of the chromosphere and corona. In addition, the sharp differences shown in Figure 3 could be hinting at the fact that the eruptive processes of solar flares may require additional physical mechanisms that are related to the magnetic topology and morphology of the solar chromosphere and corona.

<sup>6</sup><https://solis.nso.edu/0/iss/>.

<sup>7</sup>[https://www.ngdc.noaa.gov/stp/CDROM/solar\\_variability.html](https://www.ngdc.noaa.gov/stp/CDROM/solar_variability.html).

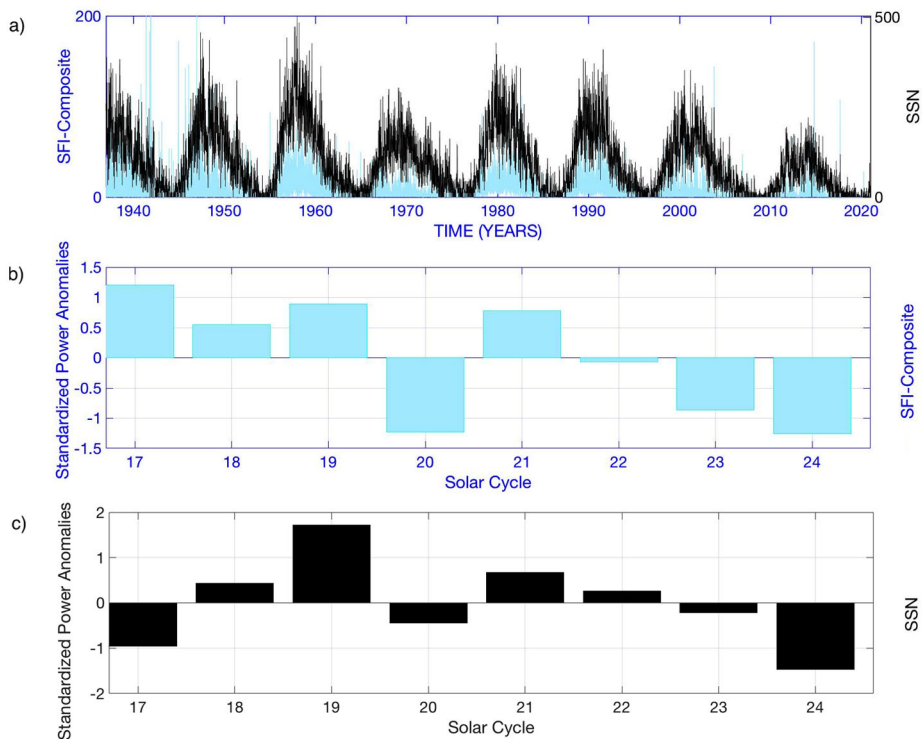


**Figure 3** Standardized power anomalies of the daily SFI composite record from 1937 to 2020. (a) Shows the comparison of the daily solar activity between the photosphere (SSN, V2 of Clette et al., 2014, in black line) and the chromosphere (composite SFI as a light blue shaded area). (b) Shows the standardized power anomalies (light blue bars) of the composite SFI for Solar Cycles 17–24. (c) Shows the standardized power anomalies (black bars) of the SSN for Solar Cycles 17–24.

Nonetheless, the overall long-term decrease in solar activity since Solar Cycle 21 in the chromospheric activity can be seen for both metrics. This is consistent with suggestions that we are at the onset of a new secular solar minimum (Velasco Herrera, Soon, and Legates, 2021).

In the solar photosphere, the sunspot activity has been observed to be weakened significantly during the secular Maunder, Dalton-Wolf, Gleissberg-Waldmeier solar minima (Velasco Herrera, Soon, and Legates, 2021; Velasco Herrera et al., 2022a). Nevertheless, the relationships between solar minimum periods and the solar chromosphere are not yet completely established. It is true that the Carrington/Hodgson event of 1859 occurs near or about the sunspot activity maximum. But given the shorter time series available, for now we should probably confine our assessments of these relationships to noting that solar flare activity at least increases and decreases in relation to the underlying magnetic activity that follows the 11-year cycles. This is another reason why it is so important to monitor the totality of solar activity tracing and tracking the photosphere, the chromosphere to the solar corona, if we are to be able to identify and quantify the nature of the new secular solar minimum that sunspot-based studies suggest has begun around 2008 (Velasco Herrera, Soon, and Legates, 2021; Velasco Herrera et al., 2022a).

### 3.2. Wavelet Analysis

In Figure 4, the wavelet spectral analysis of the SFI is shown. In order to find the patterns of the SFI variations, we spectrally analyze them with the wavelet transform. The primary time series analyzed is the daily SFI data, which is shown in the upper panel of Figure 4. The evolution of each of the periodicities of the SFI records is shown in the bottom panels.

Figure 4a shows the wavelet results of the daily SFI time series. The time-frequency wavelet spectrum (bottom panel of Figure 4a) yields the periodicities of 21.88 years, 10.94 years, 5.2 years, 3.5 years, 1.7 years, 1 year, 0.41 years (149.7 days), 0.17 years (62.1 days), and 0.07 years (25.9 days). Figure 4b shows the wavelet spectrum of the monthly SFI. The wavelet spectrum (bottom panel) shows the periodicities of 22.1 years, 11 years, 5.2 years, 3.5 years, 1.7 years, 1 year, and 0.41 years (149.7 days). Figure 4c shows the wavelet analysis of the annual SFI. The wavelet spectrum (bottom panel) shows the periodicities of 22.1 years, 11 years, 5.2 years, and 3.5 years. We note the internal consistency of the identified periodicities among the wavelet spectra for the three time series. That is, the same or very similar periodicities are found on all timescales:  $\approx 22$  years,  $\approx 11$  years, 5.2 years and 3.5 years on all three timescales; and 1.7 years, 1 year, and 0.41 years for the higher frequency timescales. Below we discuss each of these periodicities in turn. We note that Wan et al. (2020) have independently identified similar periodicities from analyzing the Purple Mountain Observatory's monthly SSN and GSN records from 1954–2011.

The  $\approx 22$ -year periodicity is related to the solar magnetic cycle (Hale cycle), and its spectral power is relatively weaker in the annual data than in the monthly and daily SFI data. The periodicity of  $\approx 11$  years is the periodicity of the solar Schwabe cycle (Schwabe, 1844). In Figure 4a–c, this periodicity is the signal with the highest spectral power. This periodicity is long-known to be present from the photosphere to the solar corona (e.g. Hathaway, 2015).

The 5.5-year periodicity is related to the energy (power) characteristics of each individual 11-year solar cycle and the asymmetry of the solar cycle is due to the intensity (power) of this periodicity (Velasco Herrera, Soon, and Legates, 2021). The most magnetically active solar cycles have higher spectral power and the least magnetically active ones have lower spectral power, consistent with this 5.5-year scale diagnostic/prognostic estimator. Velasco Herrera, Soon, and Legates (2021) recently adopted this unique insight to proffer the simultaneous hindcasts and forecasts of the sunspot activity cycles. This periodicity is a subharmonic of the 11-year solar cycle (Polygiannakis, Preka-Papadema, and Moussas, 2003; Velasco Herrera, Soon, and Legates, 2021). This periodicity has been reported in different solar indices, for example, in the sunspot number record, in group sunspot numbers, in historical aurora records, in the  $^{10}\text{Be}$  and  $^{14}\text{C}$  cosmogenic isotopes records, in polar faculae activity records (Silverman, 1992; Polygiannakis, Preka-Papadema, and Moussas, 2003; Usoskin et al., 2006; Kollath and Olah, 2009; Le Mouél, Lopes, and Courtillot, 2019, 2020; Velasco Herrera, Soon, and Legates, 2021; Velasco Herrera et al., 2022a), and now we report this 5.5-year oscillation in the SFI activity.

The various periodicities between 0.6 and 4 years are collectively categorized here as the quasi-biennial oscillation of the solar activity (QBO). Many have suggested this to be associated with solar dynamo processes (see, e.g., Howe et al., 2000; Mendoza, Velasco, and Valdés-Galicia, 2006; Obridko and Shelting, 2007; Valdés-Galicia and Velasco Herrera, 2008; Fletcher et al., 2010; Bazilevskaya et al., 2014; McIntosh et al., 2015; Bazilevskaya et al., 2016; Kiss, Gyenge, and Erdélyi, 2018; Velasco Herrera et al., 2018).

The periodicities between 1 and 2 years are the so-called mid-term periodicities (MTPs). The MTPs have already been reported in coronal hole areas (McIntosh, Thompson, and

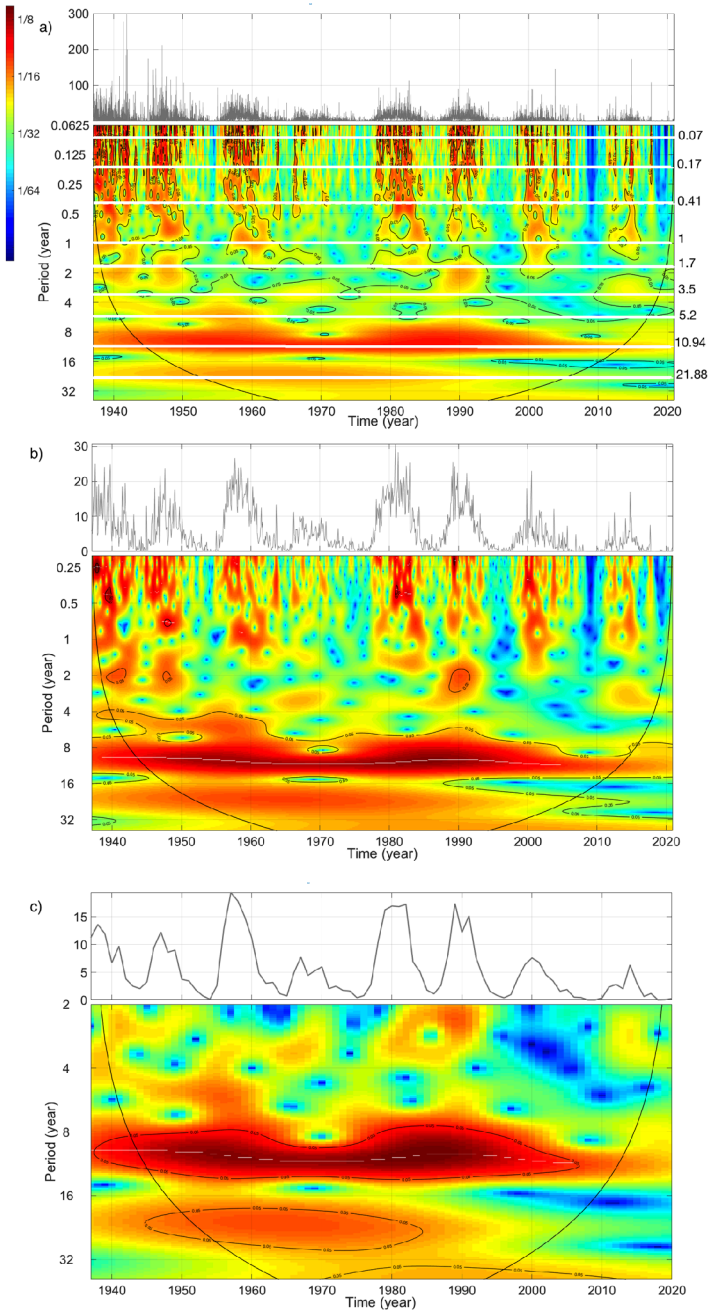


**Figure 4** Time-frequency wavelet results of the SFI: **(a)** daily, **(b)** monthly, and **(c)** annual values for Cycles 17–24 (1937–2020). The time-frequency regions with wavelet spectral power detection above 95% confidence level are marked with thin black contours. We also mark all the quasi-regular oscillations we identify and discuss in the main text for panel **(a)** using white horizontal lines across the full interval 1937–2020. The lower panels of **(a)**, **(b)**, and **(c)** show the calculated wavelet power spectral density (PSD) in normalized units adopting the red-green-blue color scales. The cone of influence (COI, U-shaped curve with shaded outer zones) shows the possible edge effects in the PSD.

Venkatesan, 1992), long duration X-ray solar emissions (Antalová, 1994), solar wind velocity (Richardson, 1944), and galactic cosmic ray intensity (Valdés-Galicia, Otaola, and Pérez-Enríquez, 1996).

Benevolenskaya (2000) suggested that the MTPs may be the result of a coupling between two specific dynamo mechanisms. The MTPs are said to be related to the strength of a high-frequency component, i.e. to the quasi-biennial periodicities produced by latitudinal or radial shears in the subsurface region of the Sun. In addition, Benevolenskaya (2000) pointed out the distinct dynamo operation producing a low-frequency component of 22 years at the tachocline associated with the large-scale radial shear of the angular velocity.

Regarding the annual periodicity, an obvious candidate for this quasi-period is the Earth orbital period. In fact, the Earth's orbital period is the most important component, at annual scale, in the analytical expansion of the Sun's position around the solar system barycenter (Bretagnon and Francou, 1988). This leads us to consider whether any of these identified periodicities could be associated with solar and planetary motions (Courtillot, Lopes, and Le Mouél, 2021).

Several authors (e.g., Cionco, 2012; Scafetta, 2012; Cionco and Soon, 2015; Stefani, Giesecke, and Weier, 2019) have shown that – based on specific forcing functions (spin-orbit couplings, tidal etc.) – several quasi-periods can be obtained, which can be phenomenologically related to solar activity modulations. For example, many of our detected quasi-periods are intriguingly similar to known periodicities associated with solar barycentric dynamics. The 3.5 year is present in the forcing terms on the solar barycentric position related to giant planets (Bretagnon and Francou, 1988; Kudryavtsev and Kudryavtseva, 2009); the 1.7-year periodicity is near the synodic period of Venus and the Earth, which is evident in the velocity and acceleration of the Sun's motion, but unimportant in the solar position (Cionco and Pavlov, 2018). Even the sub-annual quasi-periods detected can be related to planetary terms in the solar barycentric position with a rather small amplitude but persistent quasi-regular oscillation around 0.35 years (Bretagnon and Francou, 1988) and in the harmonic decomposition of the Earth's disturbing function, which is indirectly forced by the solar motion (Cionco, Kudryavtsev, and Soon, 2021).

If any of these competing planetary motion-based explanations for the MTPs hold, this would contradict Benevolenskaya's (2000) explanation. Therefore, this latter interpretation suggests that the simultaneous operation of dynamos both within the subsurface and tachocline regions of the Sun, as proposed by Benevolenskaya (2000), might be incorrect. A further argument against the simultaneous operation of two dynamos, as proposed by Benevolenskaya (2000), is the modulations of the shorter-term periodicities by the 11-year cycles, as discussed in Section 3.3 and Figures 6 and 7 below.

On the other hand, we note that the periodicity of about 1.6–1.8 years has been reported not only for photospheric and chromospheric magnetic activity (see, e.g., the results for the young solar analogue HD 30495 by Soon et al., 2019) but also for the coronal activity in three young solar analogues:  $\iota$  Horologii (Metcalf et al., 2010; Sanz-Forcada, Stelzer, and Metcalfe, 2013; Ibañez Bustos et al., 2017), KIC 10644253 (Salabert et al., 2016), and 8041424 (Montet, Tovar, and Foreman-Mackey, 2017). If these periodicities are common to multiple solar analogues, each presumably with distinct planetary systems, this might offer more support for the former explanation. Therefore, we believe the correct explanation has not yet been found.

In terms of the higher frequency periodicities, Rieger et al. (1984) first reported the periodicity of 154 days in hard X-ray solar flares. All solar indices have reported the Rieger oscillation (i.e. Gurgenshvilis et al., 2016), suggesting that the Rieger periodicity is not an exclusive feature of energetic flaring activity (Velasco Herrera and Perez-Peraza, 2010;



Gurgenashvili et al., 2016). However, it could be associated with the solar magnetic field (Gurgenashvili et al., 2016) and could indicate that the whole solar atmosphere is affected similarly, or the solar atmosphere is coupled to all solar layers, from the photosphere to the corona (Velasco Herrera and Perez-Peraza, 2010) in different periodicities (from days to years). In addition, Rieger reports on the temporal distribution of these high-energy events and finds that these events tend to occur in groups with a mean spacing of  $\approx 154$  days and are not randomly distributed in time.

The periodicity of 25.9 days is related to solar rotational modulation. This periodicity is a modulation reported from the photosphere, chromosphere, and corona (Kane, Vats, and Sawant, 2001; Kane, 2002a,b) with variations ranging from  $\approx 25$  to 31 days, probably reflecting different dominant latitudinal zones imprinting on the solar activity indices as the Sun is well-known to be a differentially rotating body. Such results appear to suggest the synchronization of solar rotation modulation persisting coherently among different solar layers.

### 3.2.1. Wavelet Coherence Between Chromospheric Activity Indices

The solar chromosphere is a highly dynamic layer of the solar plasma, so SFI and Ca II K are essentially two complementary solar chromospheric indices and individually show both general and particular characteristics of the solar chromosphere.

In Section 3.1.1 we have already compared the amplitude between these chromospheric indices (SFI and Ca II K) qualitatively. In this section we present a more quantitative comparison, i.e. we analyze the coherence of identified frequency channels between the SFI and Ca II K in the solar chromosphere.

The classical wavelet coherence (e.g. Torrence and Compo, 1998; Torrence and Webster, 1999; Velasco Herrera et al., 2018; Soon et al., 2019, for more detail about our method) is shown in Figure 5a. A broad overall coherence between SFI and Ca II K activity indices can be observed for periodicities greater than two years. The relative phase between these two solar indices is, on average, in-phase (as indicated graphically in the figures by the left to right orientation of the arrows). This indicates that any of these two solar indices can be used to analyze the chromosphere, as long as the chromospheric variability analyzed is for the 2-year or longer oscillations. This result could indicate that, although the chromosphere is a heterogeneous solar layer, periodicities greater than two years show broadly similar time-variation characteristics from the lower to the upper chromosphere.

For periodicities lower than two years, the wavelet coherence appears to be weaker, but it seems to be relatively strong during the maxima and minima of each solar cycle. This lower coherence between the two indices for the higher frequencies is perhaps due to the fact that Ca II K is an index of the high photosphere and of the low chromosphere, while the SFI is related to the explosive solar activity ultimately originated from the solar corona. That is, the SFI is an index that is probably better associated with the higher part of the solar chromosphere. So, we suggest that if researchers are interested in studying separately the low chromosphere and the high chromosphere, then Ca II K for the former and SFI for the latter would probably be more suitable.

The signal-to-noise wavelet coherence is shown in Figure 5b. As for the classic coherence analysis, the high coherence can be observed for periodicities longer than two years. However, the coherence between periodicities of 0.25 and 1 year has increased in this differently defined wavelet coherence that seeks to optimize the signal-to-noise ratio of the data series.

This new wavelet coherence metric suggests that the main difference between SFI and Ca II K lies between the periodicities of 1 and 2 years. We note that explosive solar activity

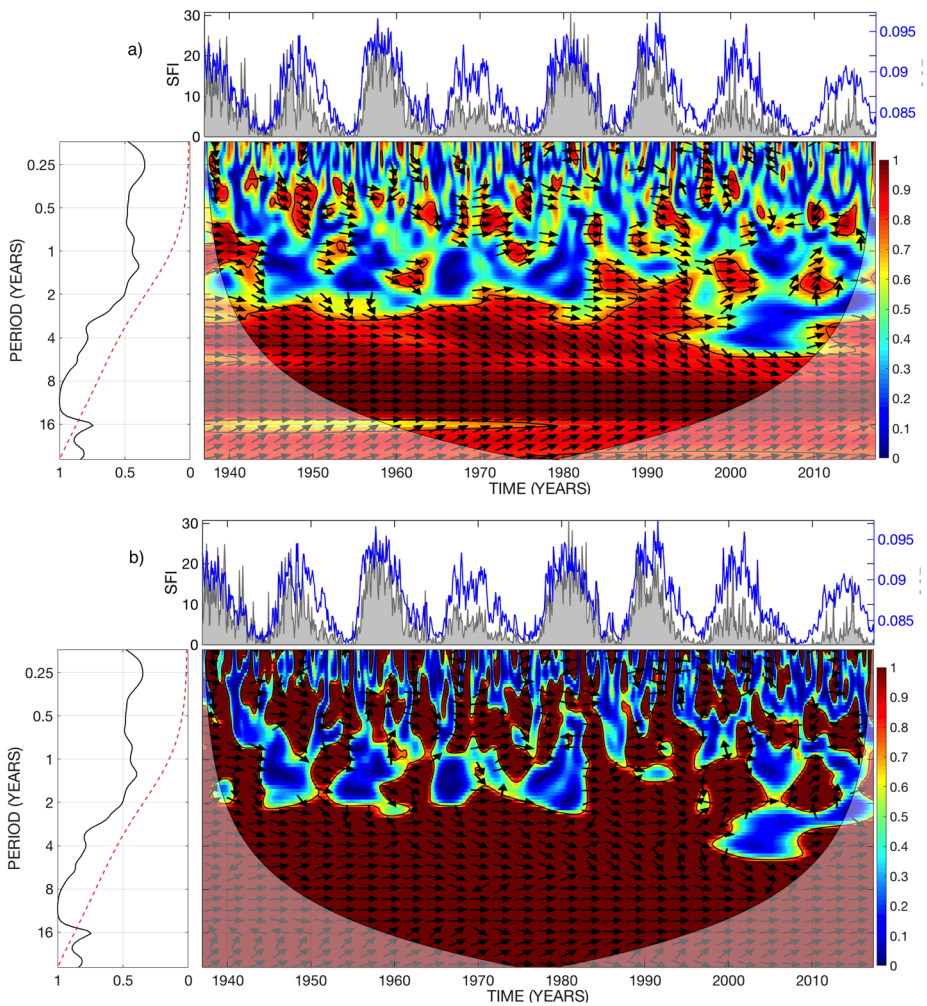


**Figure 5** Time-frequency wavelet coherence between monthly records of composite SFI (as a grey area) and the composite chromospheric Ca II K time series (in blue line): **(a)** classical coherence wavelet and **(b)** signal/noise coherence wavelet for Cycles 17–24 (1937–2020). The central panel for both **(a)** and **(b)** shows the calculated wavelet coherence power spectral density (PSD) in normalized units adopting the red-green-blue color scales. The cone of influence (COI, U-shaped curve with shaded outer zones) shows the possible edge effects in the PSD. The black arrows in the PSD indicate the relative phase between SFI and Ca II K in time-frequency domains. The orientations  $\rightarrow$  ( $0^\circ$ ) or  $\leftarrow$  ( $180^\circ$ ) indicate that there is a linear in-phase or anti-phase, synchronization, respectively, at a certain frequency between these two phenomena. Any other orientation means that there is a complex, non-linear synchronization and an out-of-phase situation, meaning that the two studied phenomena have a more complex non-linear relationship. The time-averaged global wavelet coherence is shown in the left-hand panel with the red dashed line indicating the 95% confidence level against red noise spectrum (see, e.g., Velasco Herrera et al., 2018; Soon et al., 2019, for more details about our method).

sometimes emits relativistic solar protons and these emissions occur around this frequency interval, when the protons acquire energies above 433 MeV (up to  $>10$  GeV). These types of events are known as relativistic solar particle ground-level enhancements (GLE). These



events occur and manifest roughly in the quasi-biennial oscillation of 1.7 years and it has been shown that these relativistic solar events are not the result of stochastic processes (Velasco Herrera et al., 2018). Therefore, we propose this could be a promising explanation. With that in mind, we note that the last GLE-73 event that occurred on 28 October 2021 is in accordance with the 1.7-year periodicity pointed out by, e.g., Velasco Herrera et al. (2018).

Finally, we highlight that the global coherence and signal-to-noise coherence spectra (left panels of Figure 5a and 5b) show significant or near significant (i.e. 95% confident above the red-noise spectrum) periodicities of 22.1 years, 11 years, 5.2 years, 3.5 years, 1.7 years, 1 year, 0.41 years (149.7 days), i.e. the same (or very similar in the case of  $\approx 22$  and  $\approx 11$  years) periodicities described earlier.

### 3.3. Amplitude and Phase Variations of the Composite Chromospheric Indices

We have analyzed each of the periodicities obtained with both the wavelet spectral analysis (Figure 4) and the wavelet coherence (Figure 5). Next, we study the variations of the amplitude and phase of each oscillation in detail.

Figure 6b–j shows the centered and normalized oscillations of the daily SFI composite (Figure 6a) obtained with the inverse wavelet transform.

Figure 6b shows the variation in the amplitude of the 21.88-year oscillation (Hale cycle). It can be seen that the amplitude of the Hale cycle is always present and persistent in all solar cycles, but starting from Solar Cycle 22 on its cycle amplitudes were smaller than compared to Solar Cycles 17–21. In Figure 6c the amplitude of the Schwabe cycle was nearly constant between Solar Cycles 17 and 22, but starting from Solar Cycle 23, one can see slight decreases in the amplitude of the 11-year oscillation. Figure 6d shows the Waldmeier spectral effect/rule that during the intense cycles the temporal power of the 5.2-year periodicity in the SFI is high and during the weaker solar cycles, the temporal power measured by this periodicity is low or weak.

For oscillations less than or equal to one year, it can be observed in panels g–j of Figure 6 that the amplitude is modulated. During the maxima of each solar cycle, these amplitudes reach their maximum values, while during the minima of these solar cycles, amplitudes have minimum values. This effect has been observed before in different solar indices, which is the reason why it has been proposed that the MTPs are modulated by the 11-year solar cycle (Mendoza, Velasco, and Valdés-Galicia, 2006; Valdés-Galicia and Velasco Herrera, 2008).

Figure 7 shows the phase variations of the two composite chromospheric indices. The monthly SFI time series and the composite chromospheric Ca II K time series are shown as grey areas and the blue line, respectively (Figure 7a).

Figure 7b shows the phase relation for these two chromospheric indices in the 0.25 and 2.0-year bands (i.e. the choice of this particular frequency band is based on the results and insights learned from Figure 5 presented in Section 3.2.1). The significant variability of the phase can be observed (SFI in black and Ca II K in blue lines), and the difference of the phase (dotted purple line) shows the asynchronization between these two solar indices (see the orientation of the arrows in the two central panels of Figure 5) as it varies wildly between  $\pi$  and  $-\pi$ . The phase difference can be positive, negative, and zero. Such a complex phase relation and phase mixing phenomenon has been proposed as a result of the hemispheric asymmetry in the solar flare activity (Özgülç et al., 2021).

Tentatively, we propose that a positive phase difference would indicate that the 0.25–2-year oscillation begins in the lower layers of the solar chromosphere and then continues to oscillate in its upper layers, that is, there is a temporal continuity of the 0.25–2-year band in

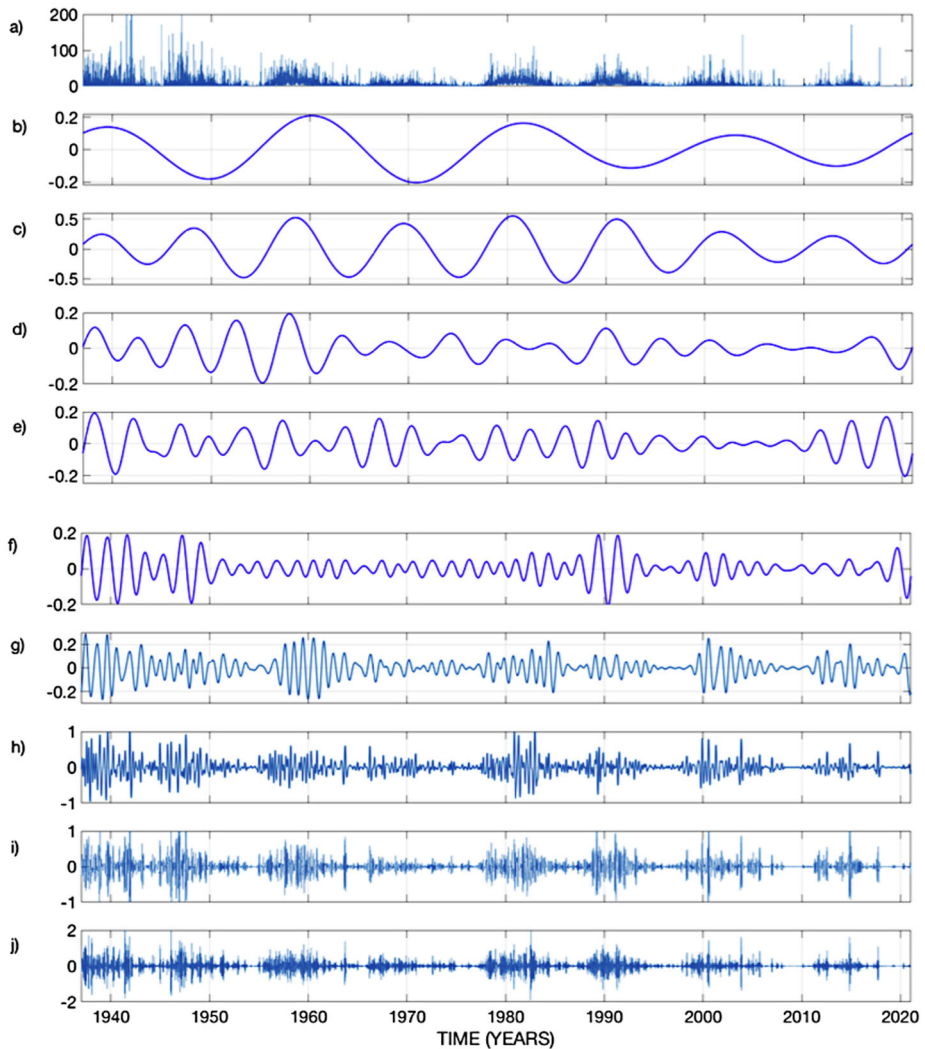


**Figure 6** Amplitude analysis of: (a) Daily SFI time series (blue line) for all the detected bandwidths or channels between 1936 and 2020 obtained with the inverse wavelet transform. (b) The 21.88-year oscillation (Hale cycle). (c) The sunspot cycle of 11 years (Schwabe cycle). (d) The 5.2-year oscillation (quasi-quinquennial cycle). (e) The oscillation of 3.5 years. (f) The oscillation of 1.7 years. (g) The oscillation of 1 year. (h) The periodicity of 0.41 years (or 149.7 days, Rieger cycle). (i) The oscillation of 0.17 years (62.1 days). (j) The oscillation of 0.07 years (25.9 days, solar rotational modulation). The centered and normalized lines represent the amplitude variations of the periodicities reported with the wavelet transform.

the solar chromosphere. A negative phase means that there may be a disconnection between the upper and lower layers of the chromosphere, so that the upper chromosphere layers oscillate before the lower chromosphere layers. A phase difference equal to zero implies a synchronization of the entire solar chromosphere.

This result shows the difference in oscillations between the lower layer and the upper chromospheric layer and may indicate a difference in the short-term magnetic energy den-

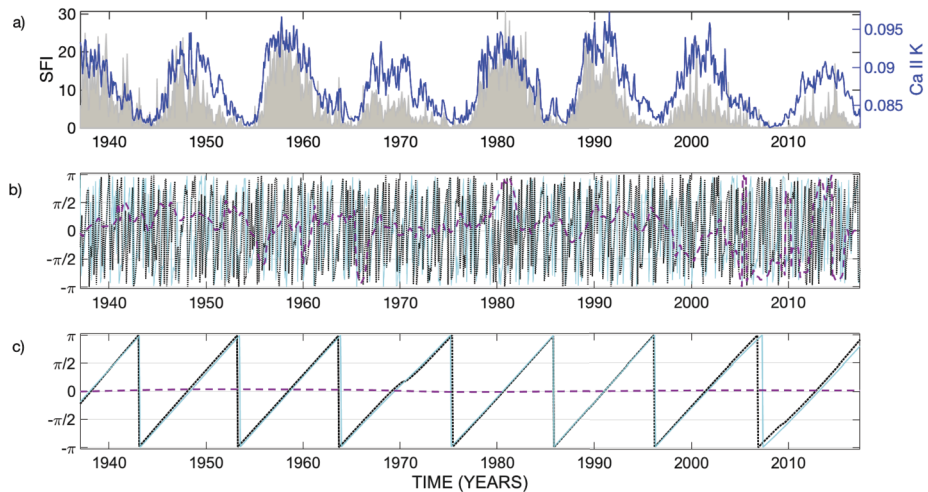


**Figure 7** Analysis of phase variations of two composite chromospheric indices. **(a)** Monthly SFI time series (as grey area) and composite chromospheric Ca II K time series (in blue line) for Cycles 17–24 (1937–2020). **(b)** Phase (continuous blue and black lines) and phase-difference (dashed purple line) for the 0.25–2.0-yr frequency band. **(c)** Phase (continuous blue and black lines) and phase-difference (dashed purple line) for the 11-year solar cycles.

sity between the lower and upper layers of the solar chromosphere. This hard-to-diagnose dynamic within the solar chromosphere appears to be recoverable from studying the phase difference between the 0.25–2-year periodicities for the upper and lower chromospheric proxies, as shown by the coherence wavelet results between these two chromospheric layers (Figure 5).

When there is a higher magnetic energy density in the lower layers of the solar chromosphere, the phase difference of the 0.25–2-year oscillation is positive and they oscillate from the lower layer to the upper layer of the chromosphere.

The disconnection (i.e. reverse energy density gradient) between the upper and lower chromosphere may occur because the energy accumulates in the upper layers of the chromosphere rooted in the original transfer of energy from the 0.25–2-year oscillations from the lower layers of the chromosphere and photosphere. Due to the energy gradient between the lower and upper layers, some of the energy returns to the lower layers. Possibly a greater amount of energy is released to the upper layers of the solar chromosphere through explosive reconnection processes and solar flares and may be extended up to the lower layers of the solar corona. Therefore, in this process of energy release in the upper chromosphere, the oscillation in the 0.25–2-year passband begins before in the lower chromospheric layer with some time delays. It has been suggested that if solar flares obtain their energy from a coronal source and flaring is one mechanism for consuming the coronal energy, then the time lag removal of energy available for flaring is about 9 months (Wheatland and Litvinenko, 2001). The phase difference between the upper and lower chromosphere shows that the time lags can be up to 12 months (Figure 7b).

Figure 7c shows the synchronization for the 11-year solar cycle between the lower and upper layers of the chromosphere. The phase difference for the 11-year periodicity (dotted purple line) for the two different chromospheric activity indices (SFI and Ca II K proxies) is strictly zero. This result indicates that the oscillation of the solar cycle passes from the lower part of the solar chromosphere (Ca II K) to its upper layers and the lower layers of the

solar corona (SFI) without much time delay. This empirical evidence indicates the transfer of energy, power, and information of the 11-year solar cycle within the solar chromosphere and the solar corona is practically instantaneous, which is in turn quite a contrast from the asynchronous relation between the upper and lower chromospheric layers on the 0.25–2-years timescales.

## 4. Conclusion

The main purpose of this article is to introduce the new composite solar chromospheric flare index, SFI, record from 1937–2020 (Figure 1). We find that the SFI activity has both similarities and differences when compared to photospheric indicators like the group sunspot numbers and sunspot numbers and even other chromospheric activity indices like the Ca II K emission and the grouped solar flares (Figure 2).

The intensity or power levels associated with each  $\approx 11$ -year solar cycle can be quantified by the power anomaly index shown in Figure 3. A possibly surprising insight from Figure 3 is that for SFI, Cycles 17, 19, and 21 were the most active flare cycles; Cycles 20, 22, 23, and 24 were the weakest, with Cycle 18 being an intermediate flare cycle. We show that this relative order of most to least active cycles is quite different from the photospheric magnetic activity indices like the sunspot numbers and group sunspot numbers.

We have performed the wavelet time-frequency analyses on the solar activity time series presented in this article in order to study any modulating signals in the data records. We find the following oscillations to be potentially relevant and physically important for the composite SFI activity record:  $\approx 22$  years,  $\approx 11$  years, 5.2 years, 3.5 years, 1.7 years, 1 year, 0.41 years (149.7 days), 0.17 years (62.1 days), 0.07 years (25.9 days) (Figure 4). We have discussed various proposed mechanisms for each of the above periodicities.

The time variations of the amplitude and phase of all these periodicities is analyzed using the inverse wavelet transform (Figures 6 and 7). In addition, we also compare the SFI activity as a recorder of the solar chromosphere to the Ca II K emission index, which is another chromospheric activity indicator (Figure 5). We have found a most interesting difference and contrast in the phase relation between the upper and lower chromospheric indicators (i.e. SFI and Ca II K indices, respectively) that depends on the oscillatory timescales or periods involved (Figure 7).

We intend to follow up the preliminary analysis of this new time series with collaborative research in a new attempt to analyze and interpret any co-variability of SFI with other available observational solar activity indices.

**Acknowledgments** The authors would like to thank all colleagues, especially Tamer Ataç and Atila Özgüç of the Kandilli Observatory, who helped to make this work possible. We thank the reviewer for the careful reading and constructive improvements to the early versions of our manuscript.

RGC acknowledges the support of the grant PID-5265TC (2019–2022) of National Technological University of Argentina. V.M. Velasco Herrera acknowledges the support from CONACyT-180148 and the support from PAPIIT-IT102420 grants. W. Soon's work was partially supported by the SAO grants with proposals ID: 000000000003010-V101 and 000000000004254-V101.

**Data Availability** The raw data supporting the conclusions of this article will be made available by the authors, without undue reservation.

## Declarations

**Conflict of Interest** The authors declare that they have no conflicts of interest.

## References

- Aguiar-Conraria, L., Azevedo, N., Soares, M.J.: 2008, Using wavelets to decompose the time-frequency effects of monetary policy. *Physica A* **387**, 2863. DOI.
- Alabiso, C.: 2015, *A Primer on Hilbert Space Theory: Linear Spaces, Topological Spaces, Metric Spaces, Normed Spaces, and Topological Groups*, Springer, Berlin. DOI.
- Antalová, A.: 1994, Periodicities of the LDE-type flare occurrence (1969–1992). *Adv. Space Res.* **14**, 721. DOI.
- Ataç, T.: 1987, Time variation of the flare index during the 21st solar cycle. *Astrophys. Space Sci.* **135**, 201. DOI.
- Ataç, T., Özgüç, A.: 2006, Overview of the solar activity during solar cycle 23. *Solar Phys.* **2**, 357. DOI.
- Bayes, T.: 1763, An essay towards solving a problem in the doctrine of chances. *Phil. Trans. Roy. Soc. London* **53**, 370. DOI.
- Bazilevskaya, G., Broomhall, A.M., Elsworth, Y., Nakariakov, V.M.: 2014, A combined analysis of the observational aspects of the quasi-biennial oscillation in solar magnetic activity. *Space Sci. Rev.* **186**, 359. DOI.
- Bazilevskaya, G., Kalinin, M.S., Krainev, M.B., Makhmutov, V.S., Svirzhevskaya, A.K., Svirzhevsky, N.S., Stozhkov, Y.I.: 2016, On the relationship between quasi-biennial variations of solar activity, the heliospheric magnetic field and cosmic rays. *Cosm. Res.* **54**, 171. DOI.
- Benevolenskaya, E.E.: 2000, A mechanism of helicity variations on the Sun. *Solar Phys.* **191**, 227. DOI.
- Bertello, L., Pevtsov, A., Tlatov, A., Singh, J.: 2016, Correlation between sunspot number and Ca II K emission index. *Solar Phys.* **291**, 2967. DOI.
- Bretagnon, P., Francou, G.: 1988, Planetary theories in rectangular and spherical variables-VSOP 87 solutions. *Astron. Astrophys.* **202**, 309.
- Camporeale, E.: 2019, The challenge of machine learning in space weather: nowcasting and forecasting. *Space Weather* **17**, 1166. DOI.
- Cappellotto, L., Orgeira, M.J., Velasco Herrera, V.M., Cionco, R.G.: 2022, Multivariable statistical analysis between geomagnetic eld, climate, and orbital periodicities over the last 500 KYR, and their relationships during the last interglacial. *Glob. Planet. Change* **213**, 1166. DOI.
- Carrington, R.C.: 1859, Description of a Singular Appearance seen in the Sun on September 1, 1859. *Mon. Not. Roy. Astron. Soc.* **20**, 13. DOI.
- Carrington, R.C.: 1863, *Observations of the Spots on the Sun from November 9, 1853 to March 24, 1861 (Made at Redhill)* Williams and Norgate, London.
- Cionco, R.G.: 2012, Potential energy stored by planets and grand minima events in comparative magnetic minima: characterizing quiet times in the Sun and stars. In: Mandrini, C.H., Webb, D.F. (eds.) *Proceedings of the International Astronomical Union, IAU Symposium* **34**, 410. DOI.
- Cionco, R.G., Soon, W.: 2015, A phenomenological study of the timing of solar activity minima of the last millennium through a physical modeling of the Sun–Planets Interaction. *New Astron.* **34**, 164. DOI.
- Cionco, R.G., Pavlov, D.A.: 2018, Solar barycentric dynamics from a new solar-planetary ephemeris. *Astron. Astrophys.* **615**, A153. DOI.
- Cionco, R.G., Kudryavtsev, S.M., Soon, W.W.-H.: 2021, Possible origin of some periodicities detected in solar-terrestrial studies: Earth’s orbital movements. *Earth Space Sci.* **8**, e2021EA001805. DOI.
- Clark, D.H., Murdin, L.: 1979, The enigma of Stephen Gray astronomer and scientist (1666–1736). *Vistas Astron.* **23**, 351. DOI.
- Clette, F., Svalgaard, L., Vaquero, J., Cliver, E.: 2014, Revisiting the sunspot number. A 400-year perspective on the solar cycle. *Space Sci. Rev.* **186**, 35. DOI.
- Connolly, R., Soon, W., Connolly, M., Baliunas, S., Berglund, J., Butler, C.J., Cionco, R.G., Elias, A.G., Federov, V.M., Harde, H., Henry, G.W., Hoyt, D.V., Humlum, O., Legates, D.R., Lüning, S., Scafetta, N., Solheim, J.-E., Szarka, L., van Loon, H., Velasco Herrera, V.M., Willson, R.C., Yan, H., Zhang, W.: 2021, How much has the Sun influenced northern hemisphere temperature trends? An ongoing debate. *Res. Astron. Astrophys.* **21**, 131. DOI.
- Courtilot, V., Lopes, F., Le Mouél, J.L.: 2021, On the prediction of solar cycles. *Solar Phys.* **296**, 21. DOI.
- Deng, H., Mei, Y., Wang, F.: 2020, Periodic variation and phase analysis of grouped solar flare with sunspot activity. *Res. Astron. Astrophys.* **20**, 22. DOI.
- Eddy, J.A.: 1974, A nineteenth-century coronal transient. *Astron. Astrophys.* **34**, 235.
- Egeland, R., Soon, W., Baliunas, S., Hall, J.C., Pevtsov, A.A., Bertello, L.: 2017, The Mount Wilson Observatory S-index of the Sun. *Astrophys. J.* **835**, 25. DOI.
- Feynman, R.P., Leighton, R.B., Sands, M.: 1963, *The Feynman Lectures on Physics, Mainly Mechanics, Radiation, and Heat I*.
- Fletcher, S.T., Broomhall, A.M., Salabert, D., Basu, S., Chaplin, W.J., Elsworth, Y., Garcia, R.A.: 2010, A seismic signature of a second dynamo? *Astrophys. J.* **718**, L19. DOI.

- Fletcher, L., Dennis, D.R., Hudson, H.S., Krucker, S., Philips, K., Veronig, A., Battaglia, M., Bone, L., Caspi, A., Chen, Q., Gallagher, P., Grigis, P.T., Ji, H., Liu, W., Milligan, R.O., Temmer, M.: 2011, An observational overview of solar flares. *Space Sci. Rev.* **159**, 19. DOI.
- Fourier, J.B.J.: 1822, *Théorie Analytique de la Chaleur, Libraires Pour Les Mathématiques, L'Architecture Hydraulique et la Marine* **24**, 569.
- Gilman, D.L., Fuglister, F.J., Mitchell, J.: 1963, On the power spectrum of "Red Noise". *J. Atmos. Sci.* **20**, 182. DOI.
- Grinsted, A., Moore, J.C., Jevrejeva, S.: 2004, Application of the cross wavelet transform and wavelet coherence to geophysical time series. *Nonlinear Process. Geophys.* **11**, 561. DOI.
- Grossmann, A., Morlet, J.: 1984, Decomposition of Hardy functions into square integrable wavelets of constant shape. *SIAM J. Math. Anal.* **15**, 723. DOI.
- Gurgenashvili, E., Zaqarashvili, T.V., Kukhianidze, V., Oliver, R., Ballester, J.L., Ramishvili, G., Shergelashvili, B., Hanslmeier, A., Poedts, S.: 2016, Rieger-type periodicity during solar cycles 14–24: estimation of dynamo magnetic field strength in the solar interior. *Astrophys. J.* **826**, 55. DOI.
- Hao, Q., Yang, K., Cheng, X., Guo, Y., Fang, C., Ding, M.D., Chen, P.F., Li, Z.: 2017, A circular white-light flare with impulsive and gradual white-light kernels. *Nat. Commun.* **8**, 2202. DOI.
- Hathaway, D.H.: 2015, The solar cycle. *Living Rev. Solar Phys.* **7**, 1. DOI.
- Hodgson, R.: 1859, On a curious appearance seen in the Sun. *Mon. Not. Roy. Astron. Soc.* **20**, 15. DOI.
- Howe, R., Christensen-Dalsgaard, J., Hill, F., Komm, W., Larsen, R.M., Schou, J., Thompson, M., Toomre, J.: 2000, Dynamic variations at the base of the solar convection zone. *Science* **287**, 2456. DOI.
- Hoyt, D.V., Schatten, K.H.: 1993, A discussion of plausible solar irradiance variations, 1700–1992. *J. Geophys. Res.* **98**, 18895. DOI.
- Hudgins, L., Friche, C.A., Mayer, M.E.: 1993, Wavelet transforms and atmospheric turbulence. *Phys. Rev. Lett.* **71**, 3279. DOI.
- Ibañez Bustos, R.V., Flores, M.G., Buccino, A.P., Saffe, C.E., Mauas, P.J.D.: 2017, Actividad cromosférica en estrellas frías. *Bol. Asoc. Argent. Astron.* **59**, 22.
- Kane, R.P.: 2002a, Periodicities in the time series of solar coronal radio emissions and chromospheric UV emission lines. *Solar Phys.* **205**, 351. DOI.
- Kane, R.P.: 2002b, Variability in the periodicity of 27 days in solar indices. *Solar Phys.* **209**, 207. DOI.
- Kane, R.P., Vats, H.O., Sawant, H.S.: 2001, Short-term periodicities in the time series of solar radio emissions at different solar altitudes. *Solar Phys.* **201**, 181. DOI.
- Kiss, T.S., Gyenge, N., Erdélyi, R.: 2018, Quasi-biennial oscillations in the cross-correlation of properties of macrospicules. *Adv. Space Res.* **61**, 611. DOI.
- Kleczek, J.: 1952, *Catalogue de L'Activité des Éruptions Chromosphériques (Première Parties)* **22**, Publ. Inst. Centr. Astron. Prague.
- Knoška, Š.: 1985, Distribution of flare activity on the solar disk in the years 1937–1976. *Contrib. Astron. Obs. Skaln. Pleso* **13**, 217.
- Knoška, Š., Letfus, V.: 1966, Catalogue of Activity of the Solar Flare 1950–1965, unpublished. The authors, VMVH and WS, have a copy of this unpublished report from Stefan Knoška.
- Knoška, Š., Petrášek, J.: 1984, Chromospheric flare activity in solar cycle 20. *Contrib. Astron. Obs. Skaln. Pleso* **12**, 165.
- Kollath, Z., Olah, K.: 2009, Multiple and changing cycles of active stars: I. Methods of analysis and application to the solar cycles. *Astron. Astrophys.* **501**, 695. DOI.
- Krauss, S., Fichtinger, B., Lammer, H., Hausleitner, W., Kulikov, Yu.N., Ribas, I., Shematovich, V.I., Bisikalo, D., Lichtenegger, H.I.M., Zaqarashvili, T.V., Khodachenko, M.L., Hanslmeier, A.: 2012, Solar flares as proxy for the young Sun: satellite observed thermosphere response to an X17.2 flare of Earth's upper atmosphere. *Ann. Geophys.* **30**, 1129. DOI.
- Kudryavtsev, S.M., Kudryavtseva, N.S.: 2009, Accurate analytical representation of Pluto modern ephemeris. *Celest. Mech. Dyn. Astron.* **105**, 353. DOI.
- Kusano, K., Iju, T., Bamba, Y., Inoue, S.: 2020, A physics-based method that can predict imminent large solar flares. *Science* **369**, 587. DOI.
- Landau, L.D., Lifshitz, E.M.: 1988 In: *The Classical Theory of Fields* **2**, Nauka, Moscow [in Russian].
- Le Mouél, J.L., Lopes, F., Courtillot, V.: 2019, A solar signature in many climate indices. *J. Geophys. Res.* **124**, 2600. DOI.
- Le Mouél, J.L., Lopes, F., Courtillot, V.: 2020, Characteristic time scales of decadal to centennial changes in global surface temperatures over the past 150 years. *Earth Space Sci.* **7**, e2019EA000671. DOI.
- Li, T., Sun, X., Hou, Y., Chen, A., Yang, S., Zhang, J.: 2022, A new magnetic parameter of active regions distinguishing large eruptive and confined solar flares. *Astrophys. J.* **926**, L14. DOI.
- Lin, J., Soon, W., Baliunas, S.L.: 2003, Theories of solar eruptions: a review. *New Astron. Rev.* **47**, 53. DOI.
- Link, F., Kleczek, J.: 1949, Influences Planétaires sur le Soleil IV. *Bull. Astron. Inst. Czechoslov.* **1**, 69.



- Livingston, W.C.: 1994, Surrogates for total solar irradiance in the solar engine and its influence on terrestrial atmosphere and climate. In: Nesme-Ribes, E. (ed.) *NATO ASI Series*, 145. DOI.
- McIntosh, P.S., Thompson, R.J., Venkatesan, D.: 1992, A 600-day periodicity in solar coronal holes. *Nature* **350**, 322. DOI.
- McIntosh, S.W., Leamon, R.J., Krista, L.D., Title, A.M., Hudson, H.S., Riley, P., Harder, J.W., Kopp, G., Snow, M., Woods, T.N., Kasper, J.C., Stevens, M.L., Ulrich, R.K.: 2015, The solar magnetic activity band interaction and instabilities that shape quasi-periodic variability. *Nat. Commun.* **6**, 6491. DOI.
- McNish, A.G.: 1937a, The atmosphere's electrical fringe. *News Serv. Bull. (Carnegie Inst. Wash.)* **4**, 151.
- McNish, A.G.: 1937b, On the ultraviolet light theory of magnetic storms. *Phys. Rev.* **52**, 155. DOI.
- Mendoza, B., Velasco Herrera, V.M.: 2011, On mid-term periodicities in sunspot groups and flare index. *Solar Phys.* **271**, 169. DOI.
- Mendoza, B., Velasco, V.M., Valdés-Galicia, J.F.: 2006, Mid-term periodicities in the solar magnetic flux. *Solar Phys.* **233**, 319. DOI.
- Metcalfe, T.S., Basu, S., Henry, T.J., Soderblom, D.R., Judge, P.G., Knölker, M., Mathur, S., Rempel, M.: 2010, Discovery of a 1.6 year magnetic activity cycle in the exoplanet host star HOROLOGII. *Astrophys. J.* **723**, L213. DOI.
- Miteva, R., Samwel, S.W.: 2022, M-class solar flares in solar cycles 23 and 24: properties and space weather relevance. *Universe* **8**, 39. DOI.
- Montet, B.T., Tovar, G., Foreman-Mackey, D.: 2017, Long-term photometric variability in Kepler full-frame images: magnetic cycles of sun-like stars. *Astrophys. J.* **851**, 116. DOI.
- Neidig, D.F., Cliver, E.W.: 1983, A Catalog of solar white-light flares (1859 – 1982), including their statistical properties and associated emissions. Air Force Geophysical Laboratory. Technical Report AFGL-TR-83-0257.
- Obridko, V.N., Shelting, B.D.: 2007, Occurrence of the 1.3-year periodicity in the large-scale solar magnetic field for 8 solar cycles. *Adv. Space Res.* **40**, 1006. DOI.
- Olah, K., Kovari, Zs., Petrovay, K., Soon, W., Baliunas, S., Kollath, Z., Vida, K.: 2016, Magnetic cycles at different ages of stars. *Astron. Astrophys.* **590**, A133. DOI.
- Orgeira, M.J., Velasco Herrera, V.M., Cappellotto, L., Compagnucci, R.H.: 2022, Statistical analysis of the connection between geomagnetic field reversal, a supernova, and climate change during the Plio-Pleistocene transition. *Int. J. Earth Sci.* **111**, 1357. DOI.
- Özgüç, A., Ataç, T.: 1989, Periodic behavior of solar flare index during solar cycles 20 and 21. *Solar Phys.* **2**, 357. DOI.
- Özgüç, A., Ataç, T.: 1994, The 73-day periodicity of the flare index during the current solar cycle 22. *Solar Phys.* **150**, 339. DOI.
- Özgüç, A., Ataç, T.: 1996, Confirmation of the 25.5-day fundamental period of the Sun using the North-South asymmetry of the flare index. *Solar Phys.* **163**, 183. DOI.
- Özgüç, A., Ataç, T., Rybák, J.: 2002, Long-term periodicities in the flare index between the years 1966–2001. In: *Proc. 10th European Solar Physics Meeting, 'Solar Variability'*, ESA SP-506, 709.
- Özgüç, A., Kilcik, A., Sarp, V., Yeşilyaprak, H., Pektaş, R.: 2021, Periodic variation of solar flare index for the last solar cycle (cycle 24). *Adv. Astron.* **8**, 5391091. DOI.
- Polygiannakis, J., Preka-Papadema, P., Moussas, X.: 2003, On signal-noise decomposition of time-series using the continuous wavelet transform: application to sunspot index. *Mon. Not. Roy. Astron. Soc.* **343**, 725. DOI.
- Richardson, R.S.: 1944, Solar flares versus bright chromospheric eruptions: a question of terminology. *Publ. Astron. Soc. Pac.* **56**, 156. DOI.
- Rieger, E., Share, G.H., Forrest, D.J., Kanbach, G., Reppin, C., Chupp, E.L.: 1984, A 154-day periodicity in the occurrence of hard solar flares? *Nature* **312**, 623. DOI.
- Salabert, D., Regulo, C., Gracia, R.A., Beck, P.G., Ballot, J., Creevey, O.L., Perez Hernandez, F., do Nascimento, J.-D., Corsaro, E., Egeland, R., Mathur, S., Metcalfe, T.S., Bigot, L., Ceillier, T., Palle, P.L.: 2016, Magnetic variability in the young solar analog KIC 10644253. Observations from the Kepler satellite and the HERMES spectrograph. *Astron. Astrophys.* **589**, A118. DOI.
- Sanz-Forcada, J., Stelzer, B., Metcalfe, T.S.: 2013, Horologi, the first coronal activity cycle in a young solar-like star. *Astron. Astrophys.* **553**, L6. DOI.
- Scafetta, N.: 2012, Does the Sun work as a nuclear fusion amplifier of planetary tidal forcing: a proposal for a physical mechanism based on the mass-luminosity relation. *J. Atmos. Solar-Terr. Phys.* **81–82**, 27. DOI.
- Schwabe, H.: 1844, Sonnen-Beobachtungen im Jahre 1843. *Astron. Nachr.* **21**, 233. DOI.
- Shibata, K., Magara, T.: 2011, Solar flares: magnetohydrodynamics processes. *Living Rev. Solar Phys.* **8**, 6. DOI.
- Silverman, S.M.: 1992, Secular variation of the aurora for the past 500 years. *Rev. Geophys.* **30**, 333. DOI.


- Song, Y., Tian, H., Zhu, X., Chen, Y., Zhang, M., Zhang, J.: 2020, A white-light flare powered by magnetic reconnection in the lower solar atmosphere. *Astrophys. J. Lett.* **893**, L13. DOI.
- Soon, W., Connolly, R., Connolly, M.: 2015, Re-evaluating the role of solar variability on northern hemisphere temperature trends since the 19th century. *Earth-Sci. Rev.* **150**, 409. DOI.
- Soon, W., Yaskell, S.H.: 2003, *The Maunder Minimum and the Variable Sun-Earth Connection*, World Scientific, Singapore.
- Soon, W., Velasco Herrera, V.M., Cionco, R.G., Qiu, S., Baliunas, S., Egeland, R.: 2019, Covariations of chromospheric and photometric variability of the young Sun analogue HD 30495: evidence for and interpretation of mid-term periodicities. *Mon. Not. Roy. Astron. Soc.* **483**, 2748. DOI.
- Stefani, F., Giesecke, A., Weier, T.: 2019, A model of a tidally synchronized solar dynamo. *Solar Phys.* **294**, 60. DOI.
- Suykens, J., Gestel, T., De Brabanter, J., De Moor, B., Vandewalle, J.: 2005, *Least Squares Support Vector Machines*, World Scientific, Singapore.
- Švestka, Z.: 1956, Several notes of the statistics of chromospheric flares. *Bull. Astron. Inst. Czechoslov.* **7**, 9.
- Torrence, C., Compo, G.: 1998, A practical guide to wavelet analysis. *Bull. Am. Meteorol. Soc.* **79**, 61. DOI.
- Torrence, C., Webster, P.J.: 1999, Interdecadal changes in the ENSO-monsoon system. *J. Climate* **12**, 2679. DOI.
- Usoskin, I., Solanki, S., Kovaltsov, G., Beer, J., Kromer, B.: 2006, Solar proton events in cosmogenic isotope data. *Geophys. Res. Lett.* **33**, L08107. DOI.
- Valdés-Galicia, J.F., Otaola, J., Pérez-Enríquez, R.: 1996, The cosmic-ray 1.68-year variation: a clue to understand the nature of the solar cycle? *Solar Phys.* **169**, 409. DOI.
- Valdés-Galicia, J.F., Velasco Herrera, V.M.: 2008, Variations of mid-term periodicities in solar activity physical phenomena. *Adv. Space Res.* **41**, 297. DOI.
- Vaquero, J.M., Vazquez, M., Sanchez Almeida, J.: 2017, Evidence of a white-light flare on 10 September 1886. *Solar Phys.* **292**, 33. DOI.
- Velasco Herrera, V., Mendoza, B., Velasco Herrera, G.: 2015, Reconstruction and prediction of the total solar irradiance: from the Medieval Warm Period to the 21st century. *New Astron.* **34**, 221. DOI.
- Velasco Herrera, V., Perez-Peraza, J.A.: 2010 Synchronization of the different solar layers. In: *38th COSPAR Scientific Assembly, 18–15 July 2010, Bremen, Germany*, 3. ADS.
- Velasco Herrera, V.M., Soon, W., Legates, D.R.: 2021, Does Machine Learning reconstruct missing sunspots and forecast a new solar minimum? *Adv. Space Res.* **68**, 1485. DOI.
- Velasco Herrera, V.M., Soon, W., Velasco Herrera, G., Traversi, R., Horiuchi, K.: 2017, Generalization of the cross-wavelet function. *New Astron.* **56**, 86. DOI.
- Velasco Herrera, V.M., Perez-Peraza, J., Soon, W., Marquez-Adame, J.C.: 2018, The quasi-biennial oscillation of 1.7 years in ground level enhancement events. *New Astron.* **60**, 7. DOI.
- Velasco Herrera, V.M., Soon, W., Hoyt, D.V., Muraközy, J.: 2022a, Group sunspot numbers: a new reconstruction of sunspot activity variations from historical sunspot records using algorithms from Machine Learning. *Solar Phys.* **297**, 8. DOI.
- Velasco Herrera, V.M., Rossello, E.A., Orgeira, M.J., Arioni, L., Soon, W., Velasco, G., la Rosique-de, C.L., Zúñiga, E., Vera, C.: 2022b, Long-term forecasting of strong earthquakes in North America, South America, Japan, Southern China and Northern India with Machine Learning. *Front. Earth Sci.* **10**, 905792. DOI.
- Wan, M., Zeng, S.-G., Zheng, S., Lin, G.-H.: 2020, Chinese sunspot drawings and their digitization – (III) quasi-biennial oscillation of the hand-drawn sunspot records. *Res. Astron. Astrophys.* **20**, 190. DOI.
- Wheatland, M.S., Litvinenko, Y.E.: 2001, Energy balance in the flaring solar corona. *Astron. J.* **557**, 332. DOI.
- Wiener, N.: 1930, Generalized harmonic analysis. *Acta Math.* **55**, 117. DOI.
- Zhang, J., Temmer, M., Gopalswamy, N., Malandraki, O., Nitta, N.V., Patsourakos, S., Shen, F., Vrsnak, B., Wang, Y., Webb, D., Desai, M.I., Dissauer, K., Dresing, N., Dumbovic, M., Feng, X., Heinemann, S.G., Laurenza, M., Lugaz, N., Zhuang, B.: 2021, Earth-affecting solar transients: a review of progresses in solar cycle 24. *Prog. Earth Planet. Sci.* **8**, 56. DOI.

**Publisher's Note** Springer Nature remains neutral with regard to jurisdictional claims in published maps and institutional affiliations.

Springer Nature or its licensor holds exclusive rights to this article under a publishing agreement with the author(s) or other rightsholder(s); author self-archiving of the accepted manuscript version of this article is solely governed by the terms of such publishing agreement and applicable law.



## Authors and Affiliations

**Victor Manuel Velasco Herrera**<sup>1</sup>  · **Willie Soon**<sup>2,3</sup> · **Štefan Knoška**<sup>4</sup> · **Jorge Alberto Perez-Peraza**<sup>1</sup> · **Rodolfo G. Cionco**<sup>5</sup> · **Sergey M. Kudryavtsev**<sup>6</sup> · **Shican Qiu**<sup>7</sup> · **Ronan Connolly**<sup>8</sup> · **Michael Connolly**<sup>9</sup> · **Michal Švanda**<sup>10</sup> · **José Acosta Jara**<sup>11</sup> · **Giovanni Pietro Gregori**<sup>12</sup>

✉ V.M. Velasco Herrera  
[vmv@igeofisica.unam.mx](mailto:vmv@igeofisica.unam.mx)

W. Soon  
[soon.willie@epss.hu](mailto:soon.willie@epss.hu)

- <sup>1</sup> Instituto de Geofísica, Radiación Solar, Laboratorio de Inteligencia Artificial, Universidad Nacional Autónoma de México, Delegación Coyoacán, 04510, Ciudad de México, Mexico
- <sup>2</sup> Institute of Earth Physics and Space Science (ELKH EPSS), 9400, Sopron, Hungary
- <sup>3</sup> Harvard-Smithsonian Center for Astrophysics, Cambridge, MA, 02138, USA
- <sup>4</sup> Tatranská Lomnica, Slovak Republic
- <sup>5</sup> Comisión de Investigaciones Científicas de la Provincia de Buenos Aires – Grupo de Estudios Ambientales, Universidad Tecnológica Nacional, Colón 332, San Nicolás 2900, Bs.As., Argentina
- <sup>6</sup> Sternberg Astronomical Institute, M. V. Lomonosov Moscow State University, 13, Universitetsky Pr., Moscow, Russia
- <sup>7</sup> Department of Geophysics, College of the Geology Engineering and Geomatics, Chang'an University, Xi'an, 710054, China
- <sup>8</sup> Center for Environmental Research and Earth Sciences (CERES), Salem, MA 01970, USA
- <sup>9</sup> Dublin, Ireland
- <sup>10</sup> Astronomical Institute of the Czech Academy of Sciences, Fričova 298, Ondřejov, 25165, Czech Republic
- <sup>11</sup> Universidad ESAN, Alonso de Molina 1652, Monterrico, Surco, Lima, 150140, Perú
- <sup>12</sup> IMM (CNR), Bologna, Italy